NANOMATERIALS SCIENCE & ENGINEERING
Vol. 2, No. 2, pp. 57-73 (2020)

RESEARCH ARTICLE

https://doi.org/10.34624/nmse.v2i2.9967

Graphoepitaxial growth of CeO_2 thin films on tilted-axes $NdGaO_3$ substrates by pulsed laser deposition

Peter B. Mozhaev[1,*], Julia E. Mozhaeva[1], Igor K. Bdikin[2], Iosif M. Kotelyanskii[3], Valery A. Luzanov[3], Jørn Bindslev Hansen[4], Claus S. Jacobsen[4]

[1] Valiev Institute of Physics and Technology of Russian Academy of Sciences, Moscow, 117218, Russian Federation
[2] TEMA-NRD, Mechanical Engineering Department and Aveiro Institute of Nanotechnology (AIN), University of Aveiro, Aveiro, 3810-193, Portugal
[3] Kotelnikov Institute of Radioengineering and Electronics of Russian Academy of Sciences, Moscow, 125009, Russian Federation
[4] Department of Physics, Technical University of Denmark, Kongens Lyngby, DK-2800, Denmark
**Corresponding author, e-mail address: pbmozh@gmail.com*

Received 6 December 2019; accepted 18 May 2020; published online 10 June 2020

ABSTRACT

Growth of CeO_2 thin films on $NdGaO_3$ tilted-axes substrates (TAS) by pulsed laser deposition (PLD) was systematically studied in a wide range of substrate tilt angles γ = 5-27º. The three-dimensional graphoepitaxial (3DGE) growth mechanism was demonstrated for all films on TAS. The observed deviations from the tangent 3DGE dependence can be divided into a systematic negative part and local deviations near certain film tilt angles. The systematic deviation may be explained as the effect of completely-strained coherent growth of the bottom layers of the CeO_2 film. The tendency of orientation of the film along the small-index crystallographic planes (012) and (013) during film growth was discovered for the first time to our knowledge. The minimization of the surface energy may account for this behavior. The width of the rocking curve and the lattice constant variation for the 3DGE CeO_2 films increase almost linearly with the substrate tilt angle until γ = 19º.

At different deposition rates the 3DGE CeO_2 film exhibits three possible structures: (i) relaxed completely oxygenated films at very low deposition rate, (ii) completely strained well-oxygenated films at moderate deposition rates, and (iii) oxygen-deficient films consisting of two layers at high deposition rates. The deviations of orientation of the film from the 3DGE formula are set by the lattice constant c in the direction normal to the (110) plane of the substrate, which, in turn, depends on oxygen deficiency and the level of strain, introduced into the film by lattice mismatch with the substrate.

1. INTRODUCTION

The tilted-axes substrates (TAS)[1] , also sometimes called vicinal, miscut, or offcut substrates, are single crystal substrates for epiaxial growth of thin films with a certain tilt between the substrate surface plane and the small-index crystallographic plane (SICP), providing conditions for epitaxial growth. This SICP is sometimes called "the habit plane", implying both usual formation of the film along this plane, and standard (not tilted) orientation of the crystal for substrate preparation.

[1] Suggested abbreviations:
TAS - tilted-axes substrate
SICP - small-index crystallographic plane
3DGE growth mechanism - three-dimensional graphoepitaxial growth mechanism
NGO - $NdGaO_3$
CMP - chemical-mechanical polishing
PLD - pulsed laser deposition
WAR-RC - rocking curve in a wide angular range
LCV - lattice constant variation

Deposition of epitaxial thin films on TAS provides unique possibilities for fine tuning of the properties of layers of anisotropic materials in planar thin film electronic devices. Application of TAS, though, have been hampered by the complexity of the film growth processes on substrates of arbitrary orientation, limiting tilt angles γ to the vicinal range (typically γ < 5º). Usual goal of deposition on TAS is improvement of the crystal quality of the film due to a change of the 3D growth mode (Volmer-Weber or Stranski-Krastanov) on the standard-oriented substrate to the 2D growth mode, usually the step-flow growth mode. Even this simple idea encountered a number of complications, one of which was a change of the film crystallographic orientation. The trivial assumption that the orientation of the epitaxial film follows the orientation of the habit plane is correct only for a minor part of the studied film-substrate combinations. One of the alternative growth mechanisms is the graphoepitaxial matching of the steps on the substrate surface, formed due to the faceting along the SICPs, and the height of the growth steps of the film. Such films demonstrate an inclination of their SICP from the habit plane, with an increasing tilt of the corresponding SICP of the film when the growth step of the film is higher than that of the substrate, and with a decreasing tilt from γ when the growth step is smaller (Fig. 1). The ratio of the heights of the growth steps sets the orientational features of the film, implying essentially three-dimensional epitaxial matching between the film and the substrate, so this growth mode may be called the three-dimensional graphoepitaxial (3DGE) growth mechanism [1].

The 3DGE mechanism was first discovered in 1971 [2] and since then numerous studies reported observation of this growth mechanism in epitaxial growth of different semiconductors, metals, oxides, and in combinations of these materials (see references in [1, 3-5]). Microscopic models explaining formation of 3DGE film-substrate relations were suggested in [2-5], but usually they may be reduced to the "geometrical model", first suggested by Nagai in 1974 [6]: the initial epitaxial relation between the film and the substrate is set by lattice matching along the substrate tilt axis, while the tilt angle of the film around this axis γ' is set by a simple formula

$$\gamma' = (c_f / c_s)\, \gamma \qquad (1)$$

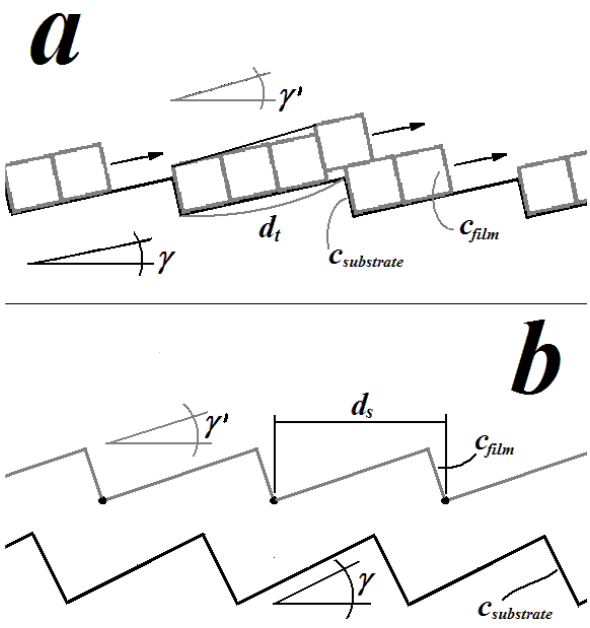

Figure 1. Simplified model of the three-dimensional graphoepitaxial (3DGE) growth of thin films on tilted-axes substrates: the inclination between the SICPs of the substrate and the film is caused by a difference between the height of the steps on the substrate surface and the growth steps of the film. The resulting tilt of the film can be higher (a) or lower (b) than the tilt of the substrate, depending on the ratio of the heights of the steps. (a) overgrowth mechanism, the tilt follows the *tangent* formula (Eq. (2) in text). (b) simultaneous seeding of the film on neighboring seeding knots (black dots) leads to the sine formula (Eq. (3)).

where c_f and c_s are the heights of growth steps of the film and the substrate, respectively. Extension of the "geometrical model" to the angles above 5º demands a change of the formula into

$$\gamma' = arctan((c_f / c_s) \cdot tan\ \gamma) \quad (2)$$

or

$$\gamma' = arcsin((c_f / c_s) \cdot sin\ \gamma) \quad (3)$$

depending on author's assumptions. Surprisingly, both variants seem to be found in different combinations of materials, with an empirical rule indicating that the *compressive* strain introduced by the SICP of the substrate into the film results in the tangent angular dependence, while the *tensile* substrate-induced strain provides 3DGE films following the sine dependence [1]. The reasons for such a difference remain unclear: the simplified models of tilt formation presented in [1] (Fig. 1a, b) do not seem convincing from any point of view. Some film-substrate combinations (namely, CeO_2/(110)$NdGaO_3$) demonstrated both dependences, for different deposition techniques and deposition conditions [1]. This ambiguous behavior may result from the very small lattice mismatch in the CeO_2 - $NdGaO_3$ combination and a very strong variation of the lattice parameter of ceria with deposition conditions, mainly oxygen partial pressure and substrate temperature.

Ceria seems to be the material which have been used to demonstrate the 3DGE growth most often of all metal oxides. A series of publications reports 3DGE growth of CeO_2 on $NdGaO_3$ (NGO) TAS with tilt around the [001] axis from the (110) SICP with e-beam evaporation, RF sputtering, and pulsed laser deposition (PLD) ([1, 7-9]). Deposition of CeO_2 on Ni tapes showed systematic 3DGE tilt of crystallites orientation in arbitrary directions [10]. Hints of 3DGE inclination of CeO_2 crystallites can be found in [11, 12], though the presented data are insufficient to make credible conclusions. The $\gamma' \approx$ 25º tilt of CeO_2 film on a (103) $SrTiO_3$ substrate (γ = 18.43º), as shown by the polar figures in [13], is in a good agreement with the 3DGE calculation (γ' = 24.8º using (2)). A tilt similar to the 3DGE growth is observed in [14], but quantitative explanation of the results demands an introduction of some interaction layer between the slopes etched in the substrate and the CeO_2 film, in a similar way to the $YBa_2Cu_3O_x$ 3DGE growth on the CeO_2 tilted-axes layers [1].

In this paper we present results of our studies of the 3DGE CeO_2 films on NGO TAS. The angular range γ = 5-18º was studied in more detail compared to the previous studies, the effect of deposition conditions on orientation and properties of the 3DGE CeO_2 films was determined.

2. EXPERIMENTAL

The TAS (5×5×0.5 mm^3) were cut from NGO single crystals, their substrate surface was set by tilting from the (110) habit plane around the [001] axis towards the (010) plane. The nominal tilt angle was varied in the range γ = 0 - 34º. Chemical-mechanical polishing (CMP) of the substrates provided flat surfaces with roughness R_a below 2 Å, as determined by AFM. Depositions were done on the as-polished substrates, without special treatment to recrystallize the surface of the substrate, only cleaning in organic solvents and 10% HCl was performed to remove contaminants present after dicing and CMP. The actual orientation of the substrate surface after CMP was checked with XRD measurements. The deviation of the actual tilt axis from the [001] axis of NGO did not exceed 5º, usually being less than 2º.

The details of the applied PLD technique can be found elsewhere [15]. Briefly, a commercially available stoichiometric high-density (>90% of bulk density) ceramic CeO_2 target was used. Most of the films in this study were deposited using the process optimized for fabrication of CeO_2 on (1 -1 0 2) sapphire substrates: T_D = 750-770 ºC, p_{O2} = 0.15 mbar, p_{total} = 0.5 mbar, energy density 1.5 J/cm^2, repetition rate 0.5 Hz [16]. This process results in rather high deposition rates, 1.2-3 Å/pulse, varying mainly with the process geometry (spot size, scan area on target, distance to substrate, etc.). In turn it demanded oxygen partial pressure p_{O2} high enough (0.15 mbar) to provide complete oxygenation of the growing film, and total pressure p_{total} of 0.5 mbar was necessary to suppress excessive bombardment of the growing film with energetic ions of the ablation plume. The CeO_2 films deposited by PLD usually grow in a mixed (001)/(111) orientation, with predominant (111) orientation when the film oxygenation is incomplete, either because of low p_{O2} and insufficient deposition temperature T_D, or due to high deposition rate [16]. At standard deposition

conditions the (111)-orientation part in CeO_2 films on (110) NGO substrates, determined with XRD measurements, was less than 0.1%, and typically (111) peaks could not be detected on the XRD θ/2θ-scans for thin (200-300 Å) fabricated films. The undesirable growth of (111) oriented films may be further suppressed by decreasing the deposition rate of CeO_2 to 0.5 Å/pulse and below. A modified deposition process with decreased energy density on target (1.1 J/cm^2) and lowered pressures (p_{O2} = 0.012 mbar, p_{total} = 0.2 mbar), resulting in a deposition rate of 0.33 Å/pulse, provided films with no signs of crystallites of (111) orientation.

No post-deposition annealing was performed; the film was cooled down to room temperature in the working atmosphere at the maximal possible rate.

The orientation and structural properties of thin films were determined using the X-ray diffraction techniques. The studies of 3DGE growth in semiconductor heterostructures showed that almost always the SICP of the film tilts around the tilt axis of TAS. To prove this behavior in CeO_2/NGO heterostructures we studied several samples with Laue diffraction, and found no deviations of the film tilt axis <110> from the substrate tilt axis [001]. The (001) plane of CeO_2 was always oriented close to the angular position of (110) NGO plane. The presence of secondary orientations was checked with rocking curves in a wide angular range (WAR-RCs), and the nature of the observed peaks was tested additionally by measurements of WAR-RC for another crystallographic plane of the film. The X-ray radiation was not monochromated or filtered with Ni filter. As a result, both sharp diffractional peaks of the broadband X-ray radiation from the SICPs of the substrate and wide diffractional peaks of

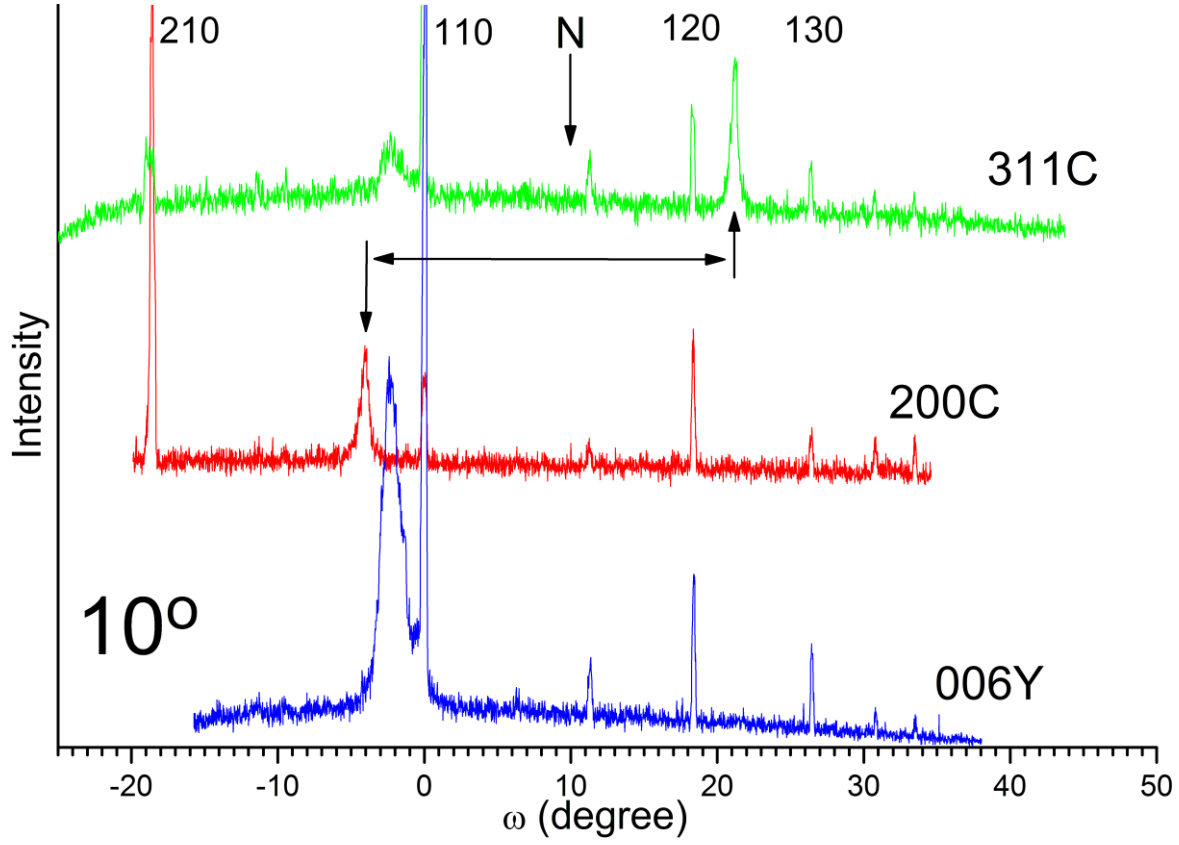

Figure 2. Determination of the orientation of 3DGE heterostructures $YBa_2Cu_3O_x/CeO_2/NdGaO_3$ with rocking curves in a wide angular range. The (110) NGO plane is tilted from the substrate plane by 10º, the position of the substrate plane is marked with "N". The broadband X-ray spectra provides peaks at the angular positions of the (210), (110), (120), and (130) SICPs of the substrate. The wide peaks from the crystallographic planes of the films are produced by the characteristic CuKα radiation at certain 2θ angular position of the detector. The additional broad peak on the top curve (ω = -3º) results from the (007) reflection of $YBa_2Cu_3O_x$ (2θ = 55º).

characteristic CuKα radiation from the SICPs of the films were observed on the same WAR-RC, providing a possibility for direct measurement of mutual inclination of the SICPs of the film and the substrate. Fig. 2 illustrates this method: a set of WAR-RCs was taken from a $YBa_2Cu_3O_x/CeO_2$/NGO heterostructure. The bottom curve corresponds to the (006) YBa_2Cu_3Ox reflection (2θ = 46.5º), the medium curve to the CeO_2 (002) peak (2θ = 33º), and the top curve - to the (113) CeO_2 peak (2θ = 56.5º). The inclination of the "(311)" peak of ~26.5º from the (001) plane of CeO_2 proves that (i) both reflections are obtained from the same part of the film, and (ii) the in-plane orientation of CeO_2 corresponds to the standard epitaxial relation for fluorite growth on $NdGaO_3$: <110>(001)CeO_2||[001](110)NGO. No other orientations of CeO_2 were detected in the sample.

The deposition rate was calibrated using lift-off removal of some part of the deposited film using a mask stable at high deposition temperature. We call the *nominal thickness* the product of the number of pulses on target and the calibrated deposition rate. The thickness was also evaluated using the Williamson-Hall method, the result was in good agreement (error below 15%) with the nominal value for CeO_2 films on a standard (110) oriented NGO substrate. The Williamson-Hall estimations of film thicknesses for simultaneously deposited samples with different tilt angles (γ = 0-12º) showed results within 10% variation from sample to sample, so we may conclude that the film growth rate is almost independent on the substrate tilt angle at least for small γ.

In addition to the crystallite size (thickness) value the Williamson-Hall method provides estimation of the *Δd/d* parameter, expressing weighted spread of the interplane distance *d* in the sample. For diffraction on the *(00l)* planes of the films with orientation close to (001) this parameter is reduced to the spread of the *c* lattice constant *Δc/c*. Sometimes *Δd/d* is called "strain", because for some epitaxial films a relation can be established between *Δd/d* and the elastic strain introduced into the film by the substrate. To avoid misunderstanding, we call the *lattice constant variation* (LCV) the *Δc/c* parameter, determined for diffraction on the *(00l)* CeO_2 planes.

The surface morphology of the films was studied with a Tencor Alfa-Step 200 profiler and a NanoSurf EasyScan AFM.

We would like to note that the main goal of fabrication of the 3DGE CeO_2 films was fabrication of YBCO/CeO_2/NGO heterostructures for the needs of another experiment (tilted-axes biepitaxial thin film structures of high-temperature superconductor YBCO, [17, 18]), so the structure and properties of the CeO_2 layer was not studied thoroughly for all fabricated films and multilayers. The θ/2θ-scans for some samples were taken in a narrow θ range or even were absent because of complications of measurements in the asymmetric diffraction geometry. These circumstances resulted in an ample collection of rocking curves measurements, providing tilt angle of the film and spread of the orientations of the crystallites of the film, but a rather moderate set of θ/2θ-scans, especially for the single CeO_2 layers before YBCO capping layer depositions. As a consequence, determination of dependences of lattice constant c and LCV is difficult and our considerations sometimes are inconclusive.

3. RESULTS AND DISCUSSION

As we mentioned above, all films showed strict alignment of the <110> axis of the film with the tilt axis of the substrate [001] NGO. The epitaxial relations were expressed as angular proximity of the (001) SICP of the film and the crystallographic plane of standard epitaxial growth (habit plane), (110) NGO, with inclination angle between the films set by the 3DGE growth relation (2).

To avoid misunderstanding we will use the following notation:

- the substrate plane is the plane of substrate surface;
- the tilt angles γ', γ are the angles between the substrate plane and the SICP of the film and the substrate, respectively;
- the inclination angle is the angle between the SICPs of the substrate and the film;
- the mis-orientation is the spread of orientations of individual crystallites of the film around the main orientation, usually determined as

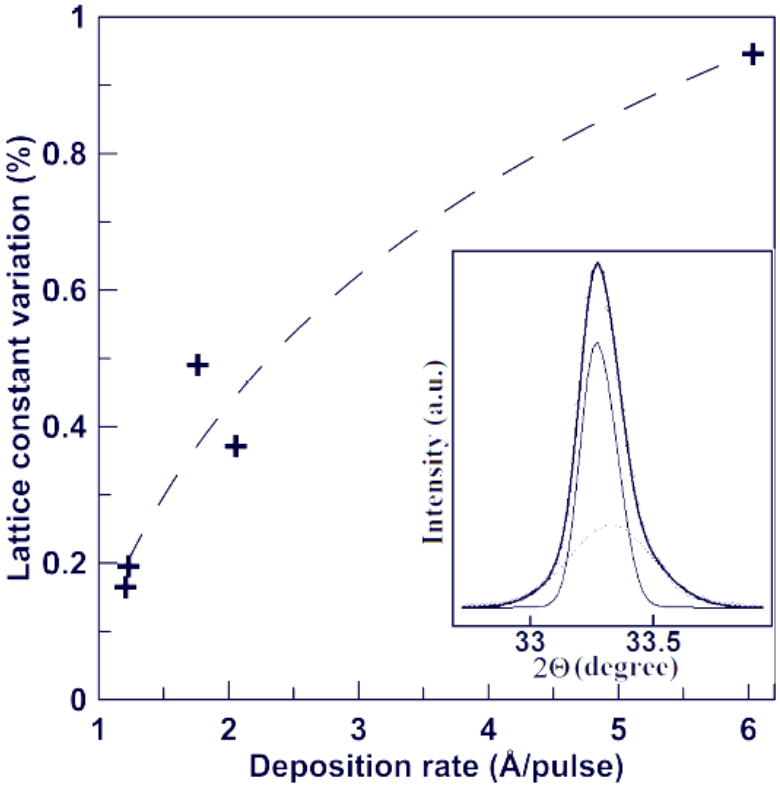

Figure 3. The lattice constant variation of CeO_2 films on (110) NGO substrates increases with deposition rate (the dashed line is a guide for the eye). Inset: the (002) peak of a thick CeO_2 film may be resolved into two peaks shifted in angular positions, implying a difference in the lattice constants for the corresponding parts of the film.

full width at half maxima (FWHM) of the corresponding rocking curve.

3.1. Standard epitaxial growth of CeO_2 films on (110) NGO substrates

CeO_2 films deposited with the standard process (deposition rate 1.2-1.8 Å/pulse for the chosen geometry of deposition) exhibited a lattice constant of 5.395-5.401 Á, close to the reference bulk value of 5.4 Á. The LCV is small, 0.1-0.5%, implying high in-depth homogeneity of the films. The width of the rocking curve for (002) peak (2θ = 33º) of the CeO_2 films on (110) NGO substrate 0.34±0.09º just slightly exceeds the FWHM of the rocking curve of the substrate (0.28±0.04º for the (440) peak at 2θ = 47º). The relatively high value of the latter results from the geometrical limitations of the measurement; at high 2θ angles (70º and more) the FWHM of the rocking curve of the substrate decreases to 0.05-0.08º, an indication of the single crystal character of the substrate. The CeO_2 peaks for this angular range are weak, making precise measurements of the rocking curves complicated.

An increase of deposition rate to 6 Å/pulse leads to an increase of lattice constant to 5.404 Å. The LCV of such films increases to ~1% (Fig. 3), manifesting non-uniform structure of thick films fabricated at high deposition rate. The X-ray θ/2θ-scans of the thick (~1500 Å) film deposited at high deposition rate allows decomposition of the (002), (004) peaks of ceria into two contributions: a narrow peak (corresponding lattice constant 5.409 Å, LCV 0.33%, estimated thickness 1290 Å) and a wide peak (5.404 Å, 0.62%, 360 Å), see inset in Fig. 3. The LCV of ~1%, estimated for the whole film, is higher than the LCV values for both film parts because the lattice constant values are different for the two parts of the film. The ratio of integral intensities of the narrow and wide peaks for the (002) peak is ~1.33, and ~0.56 for the (004) peak. This increasing "visibility" of the wide peak

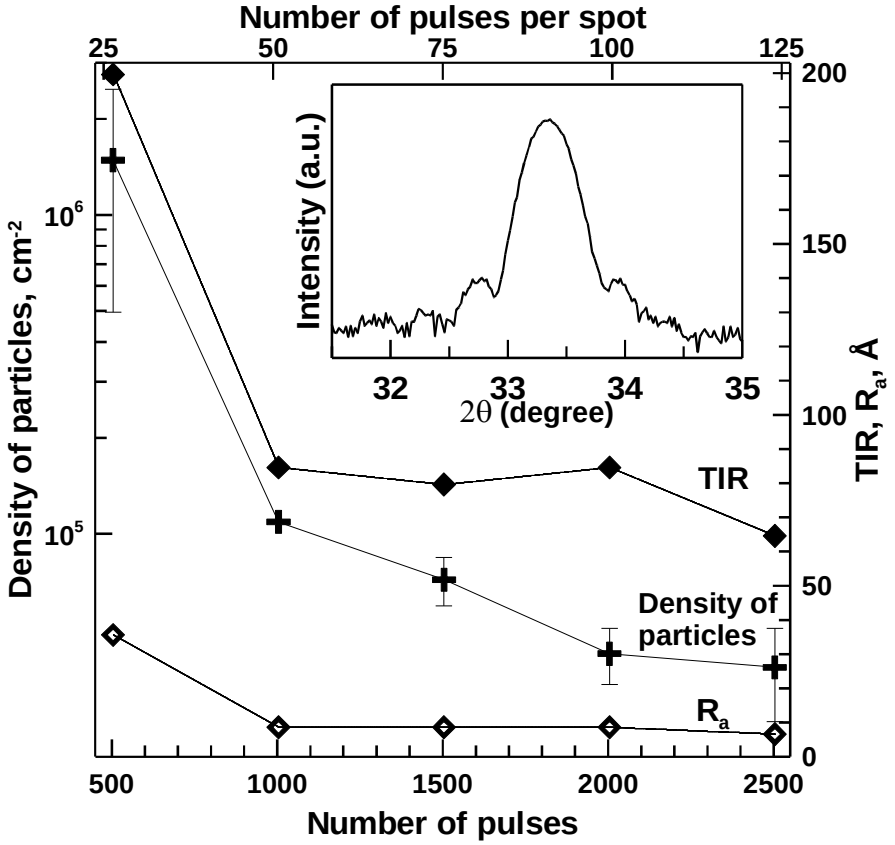

Figure 4. Evolution of parameters of CeO_2 film surface morphology (roughness, density of particles, and total range of the profiler measurement on a 100 nm scan) as a result of metallization of the target surface under laser irradiation. Inset: the CeO_2 films deposited from a ceramic target show clear Laue oscillations on the X-ray θ/2θ-scans.

for the higher measurement angle θ may be interpreted as a presence of two layers in the film, with the narrow peak corresponding to the top layer. The sum of the estimated thicknesses is close to the nominal thickness of the film, corroborating our assumption of formation of two layers. The splitting of the peaks of the θ/2θ-scans was never observed for the films grown with deposition rate of 1-2 Å/pulse, but could be detected for some of the films fabricated at 3 Å/pulse.

The observed features can be explained as the result of relaxation of the substrate-induced tensile strain. The top layer represents the relaxed part of the film over certain relaxation thickness; the value of ~350 Å is quite typical for oxide films growth. The lattice constant of the relaxed layer ~5.41 Å is higher than 5.398±0.003 Å, observed for the films deposited with low deposition rate, probably as a result of incomplete oxygenation of the film deposited at high rate. The bottom layer shows a smaller *c* value, 5.404 Å, due to the distortion generated by the substrate-induced tensile biaxial strain. Continuous relaxation of this strain with thickness, with corresponding increase of the *c* lattice constant, may be responsible for the high LCV value for the bottom layer. A relatively small distortion of the *c* lattice constant (0.2-0.5%, depending on the applied model) compared to the substrate-induced strain of ~1% implies formation of semi-coherent interface with the substrate, typical for defect fluorites.

The X-ray diffraction studies, the thickness measurements, and the AFM surface observations showed a strong dependence of properties of the CeO_2 films on the modification of the target surface (Fig. 4). Under laser irradiation the surface of CeO_2 ceramic target gains metallic glitter, probably as a result of loss of oxygen. Such metallization of the target surface significantly changes the properties

of the CeO_2 film. The deposition rate from the ceramic target is almost 1.5 times higher than from a completely developed metallized surface. The decrease of the deposition rate is very fast and takes place after just 10-15 shots per each spot on the target. The films deposited from the ceramic target show thickness fringes (Laue oscillations) on the θ/2θ-scans (see inset in Fig. 4), manifesting high smoothness of the film surface and good homogeneity of the film. At the same time, estimation of the LCV in the films prepared from the ceramic target, exhibits rather high values even at low deposition rate, e.g., 0.5% at 1.8 Å/pulse or 0.45% at 1.2 Å/pulse (compare with data from a metallized target in Fig. 3). Simultaneous observation of thickness fringes and increased LCV may be accounted for the lattice constant inhomogeneity found in the x-y plane (along the film surface), and not along the z-direction (in the films growth direction). The excessive LCV disappears after 15-20 shots per spot on the target, but the thickness fringes are still observed up to ~25 shots per spot. After 25 shots the films never demonstrate thickness fringes (for a typical peak shape for such films see inset in Fig. 3), but the evolution of surface morphology just starts (Fig. 4). The mechanisms for smoothening of the CeO_2 film surface deposited from a metallized target are outside the frame of this article and will be discussed elsewhere. They were briefly considered in the discussion of yttria nanoparticle formation in Ref. [19].

All properties, both structural and morphological, of the CeO_2 films on (110) NGO substrates, did not change after each spot on the target was irradiated with ~150 shots. Removal of the metallized layer from the surface of the target with grinding completely restores the properties of the fabricated films. To improve reproducibility of the experiment, we decided to fabricate CeO_2 films

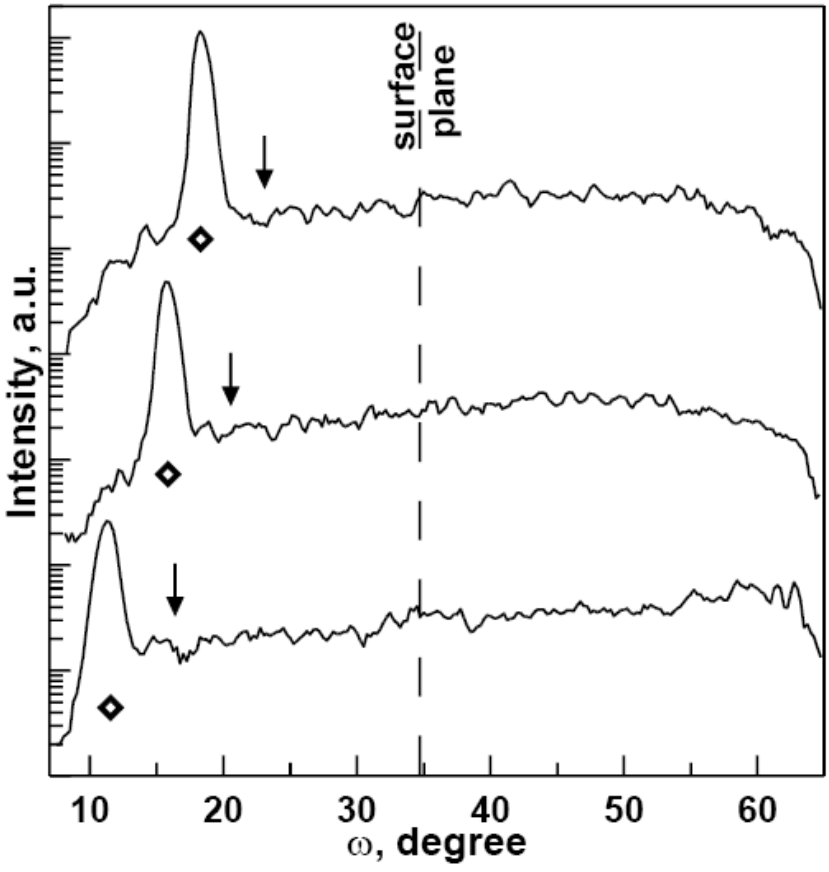

Figure 5. XRD rocking curves for the (004) CeO_2 peak of the 3DGE films on NGO TAS. The positions of the (110) planes of the substrates are marked with arrows, the substrate tilt angles are 11.4, 14, and 18.7º, from top to bottom. The (004) peaks of the CeO_2 films are marked with diamonds, the tilt angles are 16.5, 19.25 and 24.5º, in a good agreement with the geometrical model (2).

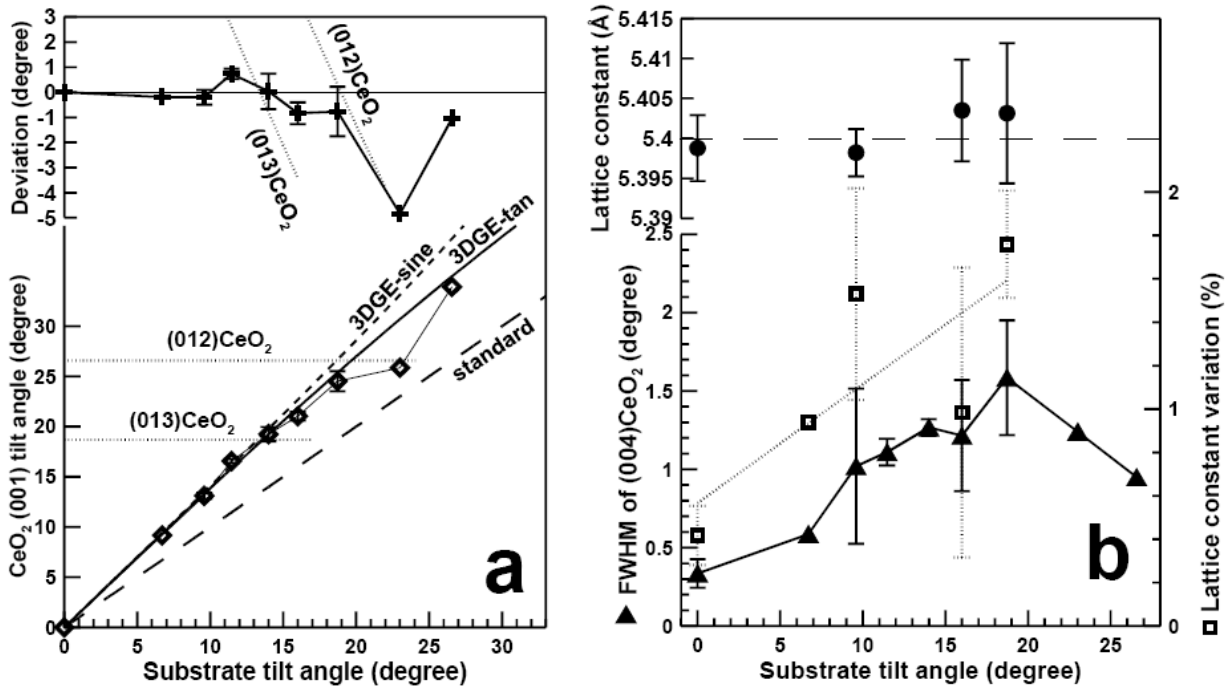

Figure 6. Angular dependences for the parameters of the 3DGE CeO_2 films on TAS NGO. a) the film tilt angle follows the 3DGE tangent dependence (2) with a small negative deviation. More intense deviations are observed in vicinity of the SICPs of the film, (013) and (012). b) Top: the lattice constant slightly increases with tilt angle. Bottom: the width of the rocking curve (triangles) increases until $\gamma \approx$ 20º, and decreases at higher angles. The LCV (squares) increases in the range 0-20º. The error bars here and on all subsequent figures are representing the spread of measured parameters of CeO_2 films.

only from a saturated metallized target, sacrificing the improved structural perfection of the films deposited from a ceramic target. Our main reason was that we have been unable to distinguish the effects of thickness and the effects of target metallization on the film properties when a ceramic target is ablated.

Summarizing, the CeO_2 films fabricated with our standard process showed good crystallinity and small mis-orientation of crystallites. An increase of deposition rate above 2 Å/pulse results in an incomplete oxygenation of the films for the chosen p_{O2} = 0.15 mbar, with development of non-uniform film as a result of relaxation of the substrate-induced strain with thickness. The metallization of the target surface complicates interpretation of the obtained results, so further depositions were performed from the saturated metallized target to avoid incontrollable changes in the deposited material.

3.2. 3DGE growth of CeO_2 films on TAS NGO

The typical rocking curves of the CeO_2 films deposited by PLD on TAS NGO are presented on Fig. 5. The (004) CeO_2 peak is shifted from the position of the (110) NGO plane towards higher tilt angles, in an agreement with the higher growth step of the CeO_2 film compared to the steps on the substrate surface (5.4 and 3.864 Å, respectively). The shift increases with the substrate tilt angle, confirming the 3DGE growth mode. A better fit of the experimental data is provided by the tangent dependence, Eq. (2).

An increase of the tilt angle γ above 30º results in an increase of the film tilt angle γ' to 45º and growth of (110)-oriented CeO_2 films for all tilt angles from 30 to 45º. The properties of the (110) CeO_2 films for the tilt angles from 30 to 45º will be presented elsewhere.

3.2.1. Angular dependences

The general dependences of the parameters of the CeO_2 3DGE films on the substrate tilt angle are

shown on Fig. 6. The orientation of all samples with varying thickness and deposited under different deposition conditions are following the same 3DGE relation (Fig. 6a). The agreement with the calculated value is good, a small systematic deviation to the smaller tilt angles may be pointed out (Fig. 6a, top). More significant deviations are observed in the vicinity of γ = 12º (positive deviation, film tilt angle $\gamma' \approx$ 17º) and γ = 23º (strong negative deviation, film tilt angle $\gamma' \approx$ 26º). One of possible explanations is a tendency to minimization of surface energy when the surface plane of the film aligns with a SICP. The positions of (013) ($\gamma' \approx$ 18.43º) and (012) ($\gamma' \approx$ 26.57º) planes are shown with dotted lines on Fig. 6a: the experimentally observed deviations are clearly attracted towards these lines. The higher intensity of the deviation at 23º may be due to a smaller sum of indexes of the (012) plane, indicating a more pronounced minimum of surface energy compared to the (013) plane.

The angular dependences of the main features of the CeO_2 3DGE films are presented on Fig. 6b. The width of the rocking curve shows a linear rise with the tilt angle until ~19º, and then a linear decrease. The lattice constant variation repeats this dependence over the range where LCV estimation was possible. Note that LCV shows a very high spread of estimated values due to the application of diverse processes with deposition rate ranging in a wide interval.

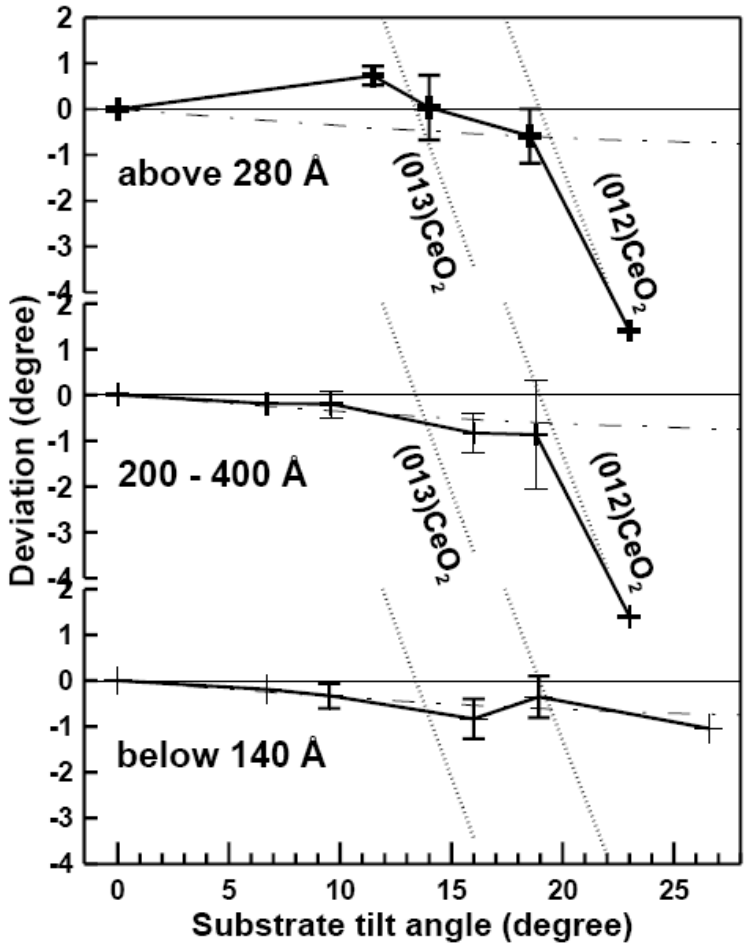

Figure 7. Evolution of the angular dependence of the deviation of the film orientation from the calculated 3DGE value. Thin films (bottom graph) follow the 3DGE tangent dependence (2) with a smaller lattice constant of the film, the corresponding calculated deviation is presented with a dash-dotted line. The films with medium thickness (middle graph) show deviation towards (012) CeO_2 orientation at substrate tilt angle of 23º. Finally, thick films (top graph) show clear deviations towards (013) and (012) CeO_2 orientations.

The lattice constant of the 3DGE CeO_2 films did not change much with the tilt angle (see Fig. 6b, top graph). The average value slightly increased for higher LCV and FWHM of the rocking curve, revealing less homogeneous films with higher density of defects in the 15-20º angular range. Usually the dominant type of defects in CeO_2 are oxygen vacancies, and an increase of their density results in an expansion of the lattice with a consequent increase of the lattice constant.

The complicated features of the general dependence of the deviation from the calculated value (Fig. 6a, top curve) may be resolved when the particular angular dependences for films of different thicknesses are presented independently (Fig. 7). The thin films show a smooth dependence with a small negative deviation increasing with the tilt angle. For the film tilt dependence on the substrate tilt angle (Fig. 6a, bottom) this would correspond to a tangent dependence (2) with a reduced film step height c_f. Such shrinking of the out-of-plane lattice constant of the growing film may result from a substrate-induced biaxial tensile strain; indeed, the NGO substrate with lattice constant of 3.864 Å (assuming pseudo-cubic lattice) introduces a tensile biaxial strain of ~1.3% into the growing CeO_2 (assuming completely oxygenated CeO_2 with lattice constant of 5.395 Å and taking into account the 45º in-plane tilt of CeO_2 axis from the <100> axes of the substrate). This strain, in the volume-preserving approximation (Poisson ratio ν = 0.5), produces a shrinking of the out-of-plane lattice constant to 5.258 Å. We have calculated the expected deviation from Eq. (2) assuming a decrease of the step height to the estimated value, and obtained an excellent agreement with the observed negative deviation of the orientation of the thin CeO_2 films from the values calculated for the saturated lattice constant (Fig. 7, dash-dotted lines). We may conclude that most probably (i) the film is seeded completely coherently strained along the (110) NGO plane, (ii) the film is completely oxygenated during seeding, the relaxed lattice constant $c_{relax} \approx 5.395$ Å, (iii) the orientation of the seed follows the tangent formula (2) exactly, and (iv) the volume of the unit cell of a completely oxygenated ceria is preserved under biaxial distortions, ν = 0.5. The latter is not the case for oxygen-deficient ceria, the usual Poisson ratio for the CeO_2 films containing oxygen vacancies is about 0.3.

An increase of the film thickness results in deviations from the initial orientation (shown as dash-dotted lines in Fig. 7). Already at ~300 Å the film on the 23º-tilted substrate turns towards the (012) CeO_2 orientation (Fig. 7, middle graph), but the overall dependence still follows the initial orientation set by the strained bottom layers of the film. Further increase of thickness results in a pronounced deviation also at film tilt of ~18.5º, corresponding to the (013) CeO_2 SICP orientation (Fig. 7, top graph).

To be fair, we must point out that we have fabricated only one sample at γ = 23º and one sample at 26.5º, so any conclusion on the angular dependences in this range is not well founded. As a consequence, a completely reliable result is presented only on the bottom graph of Fig. 7.

3.2.2. Effect of deposition rate and thickness on the properties of the 3DGE CeO_2 films

An important drawback of our study is the fact that we are not able to distinguish reliably the effect of thickness and the effect of deposition rate: a significant part of the fabricated samples differed in thickness due to the changes of the geometry of deposition, and, hence, the deposition rate.

The effect of deposition rate can be illustrated by Fig. 8. An increase of deposition rate can lead to incomplete oxygenation of the growing film, with corresponding increase of the measured *c* lattice constant. In our deposition system with p_{O2} = 0.15 mbar during the standard deposition process, complete oxygenation (lattice constant 5.395-5.397 Å) may be obtained for deposition rates below 2 Å/pulse (Fig. 8). The deposition rate of 3 Å/pulse is slightly excessive and results in a broad variation of lattice constants depending on the repetition rate (in fact, the period between the pulses), the substrate tilt angle, the film thickness, etc. The observed dependence is in an excellent agreement with our results on standard (110) NGO substrates, see Section 3.1.

The common effect of pressure and deposition rate is demonstrated by the dependence of lattice constant on the oxygen partial pressure at a relatively low deposition rate of 1 Å/pulse (see inset in Fig. 8). A decrease of oxygen partial pressure

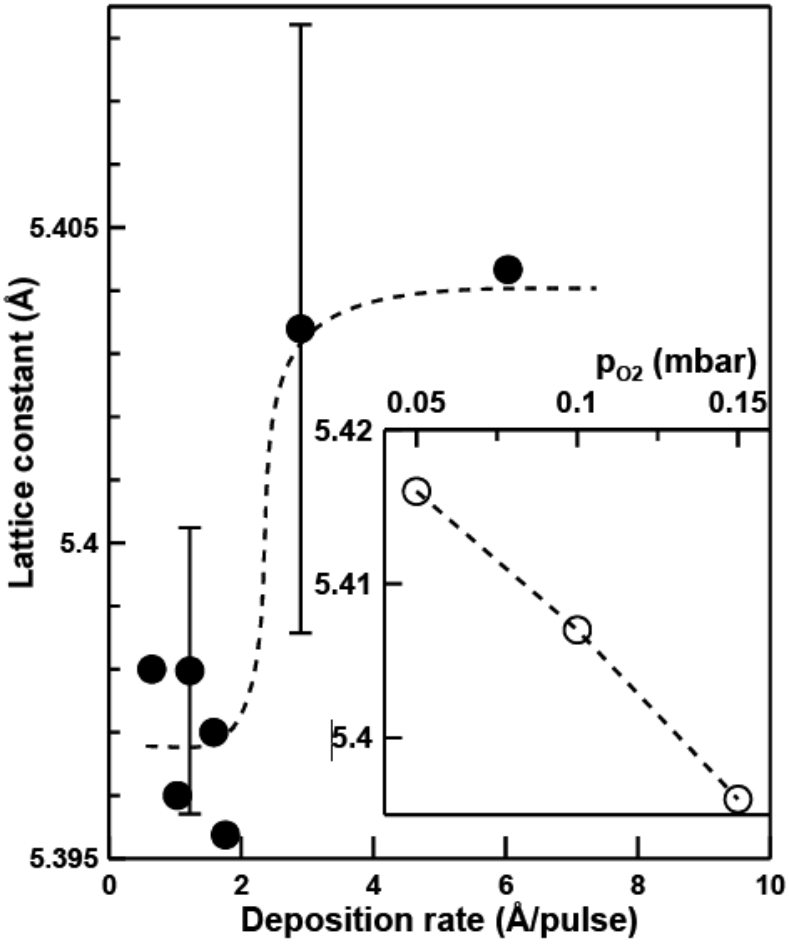

Figure 8. Lattice constant dependence on deposition rate for the 3DGE CeO_2 films, oxygen partial pressure 0.15 mbar. Inset: lattice constant dependence on oxygen partial pressure, deposition rate 1 Å/pulse.

results in a monotonous increase of the lattice constant up to 5.416 Å at p_{O2} = 0.05 mbar, implying that insufficient oxygenation is the main reason for the expansion of the c lattice constant with an increase of the deposition rate at constant p_{O2}.

The effect of thickness on the properties of the 3DGE CeO_2 films can be clarified if the samples are divided according to the deposition rates, below 2 Å/pulse and above. The data for the tilt angle 18.43º are presented in Fig. 9, the open symbols of all the graphs of Fig. 9 correspond to low deposition rate samples, while closed symbols show the features of the films grown at high deposition rate. Considering the presented results please keep in mind that we could not completely remove the dependence on deposition rate from the thickness dependences, because the thinner films were generally obtained at lower deposition rates than the more thick ones.

The deviation from the calculated film tilt value (using the standard 5.398 Å step height) for the low-rate films is small, <1º (Fig. 9a). Excluding the point at 40 Å with extremely low average deposition rate (0.4 Å/pulse × 0.1 Hz = 0.04 Å/s), we get the deviation from the calculated value almost independent on thickness and close to the value for the coherently strained ceria (-0.6º, the dash-dotted line on Fig. 9a). Taking into account the influence of deposition rate on the observed thickness dependence, we may suppose that the strain introduced into the film by lattice mismatch increases with deposition rate (revealed by an increase of thickness). This is in a good agreement with our observations for the CeO_2 films on (110) NGO substrates: the lattice constant c for slowly

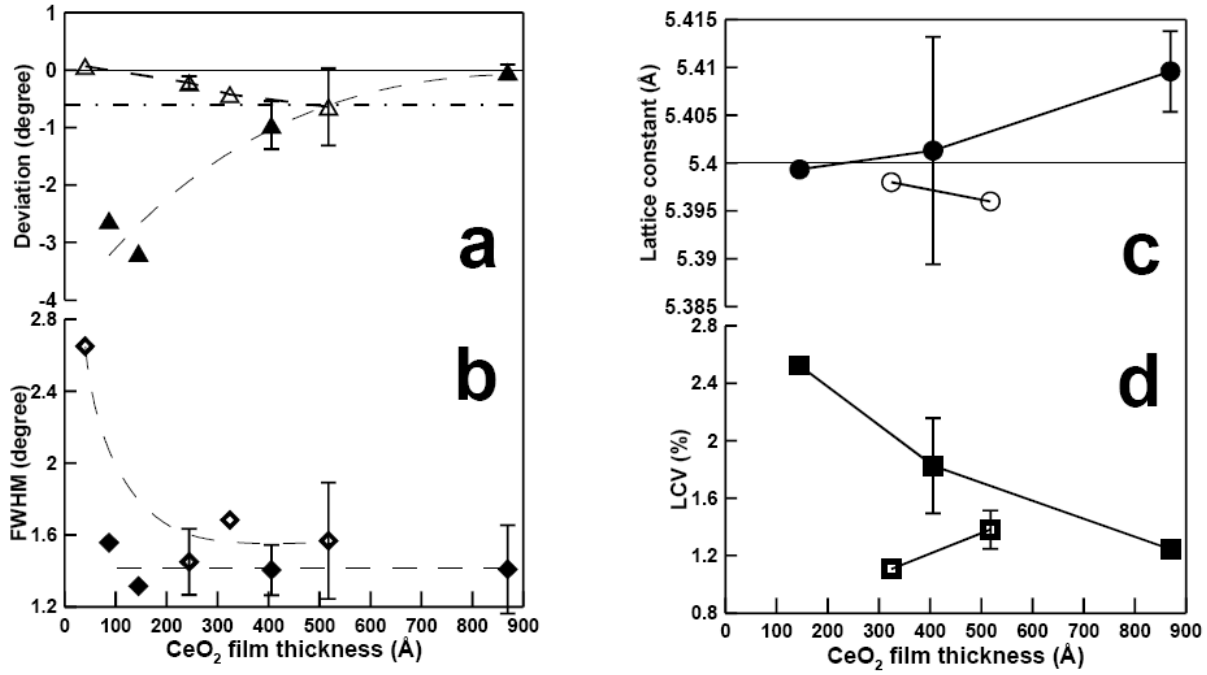

Figure 9. Thickness dependences of properties of the 3DGE CeO_2 films deposited at different deposition rates, substrate tilt angle 18.43º. Open symbols on all graphs correspond to deposition rates 1.5 Å/pulse and below, closed symbols - to deposition rates 2.5 Å/pulse and above. The lines are given as guides for the eye.

grown films is close to the standard value and the LCV is very small, down to 0.1%. These observations imply very low or negligible effect of substrate misfit, in a contrast with the films grown at high rates, with clear lattice constant contraction and relaxation of the introduced distortion with thickness. The weak bonding over the film-substrate interface at a very low deposition rate is corroborated by a very high width of the rocking curve for the film grown at the extremely low rate (Fig. 9b). All other low-rate films showed very close values of FWHM, ~1.6º (Fig. 9b). The lattice constant is small, 5.396-5.398 Å, again in a good agreement with the data on the CeO_2 films deposited on standard (110) NGO substrates at low deposition rates (Fig. 9c). The LCV, though, is significantly higher, ~1.3% (Fig. 9d), the reasons for this should be clarified additionally.

Summarizing, the 3DGE CeO_2 films deposited at low deposition rate strongly resemble the CeO_2 films grown on standard (110) NGO substrates at low rate: they are fully oxidized, with low level of substrate-induced strain. The orientation of the films is set by the contracted c due to the substrate-induced strain, but the introduced strain is decreased with lowering the deposition rate. High density of oxygen vacancies of the substrate surface during seeding may promote substrate-film bonding, explaining the observed influence of deposition rate on the level of substrate-induced strain. Another good explanation of the observed orientational behavior of the films grown at low deposition rate is enhanced relaxation at very low deposition rates. If this supposition is correct, then the relaxation periods between the laser pulses at the extremely low deposition rate is high enough to completely remove all substrate-induced strain for the first unit-cell-thick layers of the CeO_2 films, as the orientation of the film exactly corresponds to the calculated using the lattice constant of a relaxed CeO_2 film.

The behavior of the films deposited at high deposition rate is more complicated. An increase of thickness (keeping in mind the corresponding increase of deposition rate, at least for some films of the set) leads to an increase of the lattice constant (Fig. 9c), in a very good agreement with the data for the films on standard NGO substrates:

thin films show *c* =5.4 Å, but for thick films it increases to 5.41 Å. An increase of *c* with thickness is monotonous from the most thin films studied, and can be attributed to the relaxation of the substrate-induced strain with thickness. The thickness of 350-400 Å sets the border between thin and thick films (see the increased slope of the c dependence on thickness, Fig. 9c), and the high spread of the measured *c* value for this range may be referred to changing critical thickness with a deviation of the deposition parameters. The LCV dependence generally supports these considerations: the most intense change of the c lattice constant is expected for the thin films as a result of strain relaxation, and the LCV, in fact, shows highest values for the thin films. An increase of thickness over the critical results in growth of the layers with almost thickness-independent relaxed lattice constant, so the slope of the LCV dependence on thickness decreases (Fig. 9d). The LCV value for the 3DGE CeO_2 films grown at high deposition rate, is much higher than that of films on standard (110) NGO substrates, but we note that with an increase of thickness the LCV of 3DGE films decreases to 1.2%, close to the value of ~1%, obtained for the standard-oriented films of similar thickness (Fig. 3). We may assume that the spread of the c lattice constant is mainly present in the bottom part of the film, and the top, presumably relaxed, layer is more homogeneous.

The orientation of the films grown at high deposition rate strongly (up to -3º) deviates from the calculated value (Fig. 9a). We have no good explanation for this phenomena and the deviation decreases with film thickness. Assuming 3DGE mechanism of this tilt formation, we can calculate the step heights coefficient $k = c_f / c_s = 1.21$, resulting in the observed tilt angle of ~22º. The corresponding film step height c_f is ~4.68 Å, or the substrate step height should change to 4.47 Å. No obvious matches were found for these translational distances in the family of (Nd,Ga,Ce)Ox oxides, so probably this tilt is not a result of chemical interaction between the film and the substrate. An increase of thickness, though, brings the film orientation into the usual 3DGE range (completely strained growth with a small negative deviation), and for thicknesses ~800 Å the film orientation reaches the "standard" value calculated using Eq. (2) (Fig. 9a). The surface of the growing film in a multilayer structure inherits the system of steps from the bottom layer - and from the substrate surface - so the orientation of the top layer follows the formula (2) as if the top layer is deposited directly on the substrate surface (see, for example, the $YBa_2Cu_3O_x/BaZrO_3/NdGaO_3$ heterostructures in [1]), if the growth mechanism is limited to the 3DGE mode and no secondary effects influence the multilayer. This inheritance of the steps on the surface explains evolution of the 3DGE CeO_2 film orientation with thickness: the top relaxed layer grows over the bottom strained layer with the same 3DGE matching relations, transforming tilt of the strained film (step height c_f = 5.258 Å) into the tilt of the relaxed film (c_f = 5.41 Å, taking into account oxygen depletion at high deposition rate). The mis-orientation of the crystallites of the films grown at high deposition rate is somewhat smaller (~1.4º) than for the low-rate films, but also remains almost constant for all thicknesses (Fig. 9b, closed symbols). This confirms our assumption of 3DGE mechanism of change of film tilt with thickness: the spread of orientations of the crystallites of the film is set by initial seeding, and then all crystallites tilt with the change of the step height in a uniform manner, conserving the overall spread of crystallites orientations and, hence, the measured FWHM of the rocking curve.

The common (thickness + deposition rate) nature of the dependences of Fig. 9 can be illustrated by the points at ~500 Å. The samples with this thickness were deposited to the highest thickness among the low-deposition-rate samples, but, at the same time, they were deposited at the highest deposition rates in this group of samples. As a consequence, the points at ~500 Å can be added to the high-rate data on Figures 9a, b, d, without significant discrepancy with the observed dependences, and even on Fig. 9c the measured c value lays withins the high spread of measured lattice constants for the high-rate samples with thickness of 400 Å.

The saturation of the growing film with oxygen depends not just on the momentary deposition rate during PLD, but also on the relaxation time as given by the period between the laser pulses. This is illustrated by Fig. 10, where a decrease of the repetition rate from 1 to 0.3 Hz at a constant momentary deposition rate of 3 Å/pulse results in a change from formation of a film with a significant

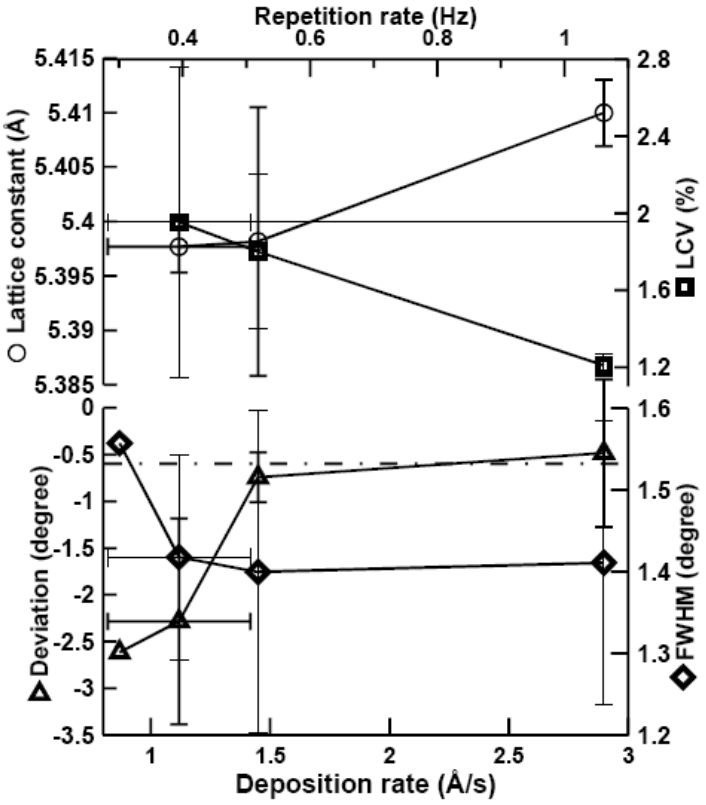

Figure 10. Dependences of properties of 3DGE CeO_2 films on the average deposition rate. Standard deposition conditions, the substrate tilt angle 18.43º, the momentary deposition rate is 3 Å/pulse. The data at 0.4 Hz (1.12 Å/s) are complemented with two samples from other data sets with similar momentary deposition rate and thickness parameters.

density of oxygen vacancies (lattice constant 5.41±0.025 Å) to the growth of an almost completely oxygenated film (5.398 Å).

Again, we cannot completely resolve the effects of deposition rate and thickness; the samples fabricated at 0.5 Hz (1.45 Å/pulse) are ~300 Å thick, while samples with a lower repetition rate are thinner and with a higher repetition rate are more thick. As a consequence, the dependences on repetition rate in general repeat the thickness dependences of Fig. 9, high-rate samples. This additionally refined data set still provides some more information on the growth of the 3DGE CeO_2 films. The ~300 Å thickness, similarly to the films on (110) NGO substrates, seems to be the border between two layers of the film. The thin films show higher mis-orientation of crystallites and a strong deviation from the calculated 3DGE orientation. Both effects gradually decrease with thickness and at the critical thickness the deviation reaches the level typical for the completely strained films (dash-dotted line, bottom graph of Fig. 10), while FWHM saturates at ~1.4º. The lattice constant below the critical thickness seems to be almost constant; we attribute this to the complex effect of more complete oxygenation, decreasing c value, and of more complete relaxation during longer periods between the laser pulses, providing lower level of the substrate-induced strain and, hence, smaller contraction of c lattice constant. The effect of the substrate-induced strain cannot be neglected, as can be seen from the LCV dependence: the variation of the lattice constant is higher for thin films, revealing relaxation of the strain with thickness. The spread of the LCV parameter from sample to sample (error bars on Fig. 10) rapidly decreases with thickness, implying reproducible growth of a relaxed CeO_2 from the critical thickness of the film.

Summarizing, the thickness dependences reveal three possible structures of the 3DGE CeO_2 films, depending on the deposition rate:

• very low deposition rate: the film grows completely oxygenated and relaxes all strain introduced by substrate mismatch in the very beginning of deposition. As a consequence, the orientation of the film corresponds to the 3DGE formula with relaxed c, but the crystallites of the film are strongly mis-oriented (the FWHM is up to 2.6º);
• low deposition rate: the film is completely oxygenated, and grows completely-strained, with a significant contraction of the c lattice constant due to the biaxial tensile substrate-induced strain. The orientation of the film follows the 3DGE relation with contracted *c* as the step height of the film, the spread of the crystallites orientations is independent on thickness in the studied range and shows much smaller values than that of the films grown at very low deposition rate;
• high deposition rate: the film presumably consists of a strained bottom part and the relaxed top layer, with a critical thickness about 300 Å. The lattice constant of the relaxed part reveals insufficient oxygenation of the film during growth. The orientation of the film evolves with thickness from a very high negative deviation for thin films, through the orientations typical for the completely-strained films at medium thickness, and to the orientation well matching the 3DGE relation for the step height equal to the lattice constant of the relaxed film. The mis-orientation of crystallites decreases with thickness and saturates at critical thickness at a level somewhat smaller than that of the low-rate films.

4. CONCLUSIONS

In summary, the deposition of CeO_2 thin films on NGO TAS by PLD usually results in the formation of tilted-axes films with the tilt angle following the 3DGE tangent dependence. The deviations from the geometrical formula can be divided into a systematic negative part and local deviations around certain film tilt angles. The width of the rocking curve and the lattice constant variation for the 3DGE CeO_2 films increase almost linearly with tilt angle until γ = 19º (film tilt $\gamma' \approx$ 24º).

The systematic deviation is present already for very thin films and may be explained as the effect of completely-strained coherent growth of the bottom layers of CeO_2 film on the NGO substrate. The biaxial distortion of the CeO_2 lattice results in contraction of the out-of-plane lattice constant c, with corresponding decrease of the growth step and the tilt angle of the film. A simple volume-preserving assumption provides excellent agreement with the measured values.

The minimization of the surface energy when the film surface is aligned with a SICP, namely, (012) at γ' = 26.6º and (013) at 18.4º, may be proposed as an explanation for the local deviations from the calculated dependence.

The macroscopic structure of the 3DGE CeO_2 films generally repeats the structure of the CeO_2 films on the standard (110)-oriented NGO substrates. The deposition rate influences the growth of 3DGE CeO_2 films in two ways: an increase of deposition rate results in an insufficient oxygenation of the Ce atoms arriving of the substrate surface, while a decrease of deposition rate provides more time for relaxation of the substrate-induced strain in the film. As a consequence, at different deposition rates the film exhibits three possible structures: (i) relaxed completely oxygenated film at very low deposition rate, (ii) completely strained well-oxygenated film at moderate deposition rates, and (iii) oxygen-deficient film consisting of two layers at high deposition rates. The deviations of orientation of the film from the 3DGE formula are set by the lattice constant c in the direction normal to the (110) SICP of the substrate, which, in turn, depends on oxygen deficiency and the level of strain, introduced into the film by lattice mismatch with the substrate.

ACKNOWLEDGMENTS

The work was supported by Program of Ministry of Science and Higher Education of Russian Federation. I.K.B. wishes to acknowledge FCT for its financial support (grant IF/00582/2015).

REFERENCES

[1] P. B. Mozhaev, J. E. Mozhaeva, A. V. Khoryushin, J. Bindslev Hansen, C. S. Jacobsen, I. K. Bdikin, I. M. Kotelyanskii, V. A. Luzanov, Three-dimensional graphoepitaxial growth of oxide films by pulsed laser deposition, *Phys. Rev. Materials*, **2** 103401 (2018).
[2] O. Igarashi, Crystallographic Orientations and Interfacial Mismatches of Single-Crystal CdS Films Deposited on Various Faces of Zinc-Blende-Type Materials, *J. Appl. Phys.* **42,** 4035-4043 (1971).

[3] M. Aindow and R.C. Pond, On epitaxial misorientations, *Philos. Mag. A*, **63**, 667-694 (1991).
[4] F. Riesz, Crystallographic tilting in lattice-mismatched heteroepitaxy: A Dodson–Tsao relaxation approach, *J. Appl. Phys.* **79,** 4111-4117 (1996).
[5] J. P. Hirth and R. C. Pond, Strains and Rotations in Thin Deposited Films. *Philos. Mag.*, **90**, 3129-3147 (2010).
[6] H. Nagai, Structure of vapor-deposited $GaxIn_{1-x}As$ crystals, *J. Appl. Phys.* **45**, 3789-3794 (1974).
[7] I. K. Bdikin, P. B. Mozhaev, G. A. Ovsyannikov, F. V. Komissinskii, I. M. Kotelyanskii, and E. I. Raksha, The growth and domain structure of YBa2Cu3Ox films on neodymium gallate substrates with a deviation of the normal to the surface from the [110] direction in NdGaO3, *Phys. Solid State*, **43**, 1611-1620 (2001).
[8] I. K. Bdikin, P. B. Mozhaev, G. A. Ovsyannikov, P. V. Komissinski, and I. M. Kotelyanskii, Growth and domain structure of YBa2Cu3Ox thin films and YBa2Cu3Ox/CeO2 heterostructures on tilted NdGaO3 substrates, *Physica C*, **377**, 26-35 (2002).
[9] P. B. Mozhaev, J. E. Mozhaeva, I. K. Bdikin, I. M. Kotelyanskii, V. A. Luzanov, J. Bindslev Hansen, C. S. Jacobsen, and A. L. Kholkin, Out-of-substrate plane orientation control of thin YBa2Cu3Ox films on NdGaO3 tilted-axes substrates, *Physica C*, **434**, 105-114 (2006).
[10] J. D. Budai, W. Yang, N. Tamura, J.-S. Chung, J. Z. Tischler, B. C. Larson, G. E. Ice, Ch. Park, and D. P. Norton, X-ray microdiffraction study of growth modes and crystallographic tilts in oxide films on metal substrates, *Nature Mater.*, **2**, 487-492 (2003).
[11] V. F. Solovyov, K. Develos-Bagarinao, D. Nykypanchuk, Nanoscale abnormal grain growth in (001) epitaxial ceria, *Phys Rev B*, **80,** 104102 (2009).
[12] R. Lyonnet, A. Khodan, A. Barthelemy, J.-P. Contour, O. Durand, J.L. Maurice, D. Michel, J. De Teresa, Pulsed Laser Deposition of $Zr_{1-x}Ce_xO_2$ and $Ce_{1-x}La_xO_{2-x/2}$ for Buffer Layers and Insulating Barrier in Oxide Heterostructures, *J. of Electroceramics* **4,** 369-377 (2000).
[13] M.A.A.M. van Wijck, M.A.J. Verhoeven, E.M.C.M. Reuvekamp, G.J. Gerritsma, D.H.A. Blank, H. Rogalla, CeO2 as insulation layer in high Tc superconducting multilayer and crossover structures, *Appl. Phys. Lett.* **68,** 553-555 (1996).
[14] P.C. McIntyre, B.P. Chang, N. Sonnenberg, M.J. Cima, Defect Formation in Epitaxial Oxide Dielectric Layers Due to Substrate Surface Relief, *J. of Electronic Mater.*, **24,** 735-745 (1995).
[15] P. B. Mozhaev, A. V. Khoryushin, J. E. Mozhaeva, J.-C. Grivel, J. Bindslev Hansen, C. S. Jacobsen, Pulsed Laser Deposition of YBa2Cu3Ox with Scanning Beam: Target to Substrate Composition Transfer and Film Structure, *J. Supercond. Novel Magnetism,* **30**, 2401-2428 (2017).
[16] P.B. Mozhaev, G.A. Ovsyannikov, J.L. Skov, Influence of laser ablation parameters on buffer CeO2 layer on sapphire orientation and on superconducting YBa2Cu3Ox thin film properties, *Technical Physics (Zhurnal Tehnicheskoj Fizika),* **44,** 242-245 (1999).
[17] P.B. Mozhaev, J.E. Mozhaeva, C.S. Jacobsen, J. Bindslev Hansen, I.K. Bdikin, V.A. Luzanov, I.M. Kotelyanskii, S.G. Zybtsev, Bi-epitaxial YBa2Cu3Ox Thin Films on Tilted-axes NdGaO3 Substrates with CeO2 Seeding Layer, *Proceedings of EUCAS'05, IOP Conf Series*, **v. 43**, iss. 1, pp. 1119-1122 (2006).
[18] P.B. Mozhaev, J.E. Mozhaeva, I.K. Bdikin, I.M. Kotelyanskii, V.A. Luzanov, S.G. Zybtsev, J. Bindslev Hansen, C.S. Jacobsen, Out-of-plane tilted Josephson junctions of bi-epitaxial YBa2Cu3Ox thin films on tilted-axes NdGaO3 substrates with CeO2 seeding layer, Proceedings of WWS'05, *Physica C*, **v. 435**, pp. 23-26 (2006).
[19] A.V. Khoryushin, P.B. Mozhaev, J.E. Mozhaeva, I.K. Bdikin, Y. Zhao, N.H. Andersen, C.S. Jacobsen, J.B. Hansen, Substrate decoration for improvement of current-carrying capabilities of YBa2Cu3Ox thin films, *Physica C*, **486,** 1-8 (2013).